http://dx.doi.org/10.5012/bkcs.2014.35.5.1440

Absorbtion Spectroscopy, Molecular Dynamics Calculations, and Multivariate Curve Resolution on the Phthalocyanine Aggregation

Davood Ajloo,[†,‡,*] Maryam Ghadamgahi,[†] Freshte Shaheri,[†] and Kobra Zarei[†]

[†]*School of Chemistry, Damghan University, Damghan 367164167, Iran*
[‡]*Department of Physical Chemistry, School of Chemistry, College of Science, University of Tehran, Tehran, Iran*
[*]*E-mail: ajloo@du.ac.ir*
Received November 5, 2013, Accepted January 21, 2014

Co(II)-tetrasulfonated phthalocyanine (CoTSP) is known to be aggregated to dimer at high concentration levels in water. A study on the aggregation of CoTSP using multivariate curve resolution analysis of the visible absorbance spectra over a concentration range of 30, 40 and 50 μM in the presence of dimethyl sulfoxide (DMSO), dimethyl formamide (DMF), acetonitrile (AN) and ethanol (EtOH) in the concentration range of 0 to 3.57 M is conducted. A hard modeling-based multivariate curve resolution method was applied to determine the dissociation constants of the CoTSP aggregates at various temperatures ranging from 25, 45 and 65 °C and in the presence of various co-solvents. Dissociation constant for aggregation was increased and then decrease by temperature and concentration of phthalocyanine, respectively. Utilizing the vant Hoff relation, the enthalpy and entropy of the dissociation equilibriums were calculated. For the dissociation of both aggregates, the enthalpy and entropy changes were positive and negative, respectively. Molecular dynamics simulation of co-solvent effect on CoTSP aggregation was done to confirm spectroscopy results. Results of radial distribution function (RDF), root mean square deviation (RMSD) and distance curves confirmed more effect of polar solvent to decrease monomer formation.

Key Words : Phthalocyanine, Solvent effect, Molecular dynamics simulation, Multivariate curve resolution, Spectroscopy

Introduction

Metal phthalocyanines are interesting macromolecules because of their high coloring property, chemical inertness, very high thermal stability, electrical conductivity, photoconductivity and catalytic activity.[1-4] They have potential applications in many areas such as in printing inks, catalysis, display devices, data storage, chemical sensors, solar cells, photodynamic cancer therapy, organic light emitting devices and photonic devices.[5,6] Metallophthalocyanine (MPc) complexes tend to aggregate in solution[7-9] and aggregation diminishes the photosensitising ability of MPc complexes.

Due to their strong and long wavelength absorption, highly efficient reactive oxygen species generation and ease of chemical modification, phthalocyanines have emerged as a promising class of second-generation photosensitizers for photodynamic therapy. Phthalocyanine forms complexes with a wide variety of metals such as Cu, Zn, Co and Ni.[10-12] Likewise photophysical and photochemical properties of metal phthalocyanines carrying various substituents have been reported in the previous literatures.[13,14]

Solvents have profound effect on phthalocyanine aggregation. Organic solvents are known to reduce aggregation whereas aqueous solvents result in aggregated complexes. However, many phthalocyanine complexes remain aggregated even in non-aqueous solutions.[15-17] Aromatic solvents such as benzene or toluene are known to give narrow Q bands in phthalocyanines spectra whereas broadening is observed in other non-aromatic solvents. Solvents also affect the photophysical and photochemical properties of MPc complexes.[18,19] Identifying different species existing in the equilibria that cannot be isolated is one of the most challenging problems in analytical chemistry. When the compounds involved in the chemical reaction have distinct spectral responses, the analysis will be straightforward. However, in many cases, the spectral responses of two or more components overlap considerably and the analysis of their mixture can no longer be performed by classical analytical methods. On the other hand, chemometric analysis of the spectral data helps chemists to obtain analytical information from the chemical system under study.[20,21] This is accompanied by the development of instruments delivering multivariate data (such as diode array detectors, fast scanning spectrometers in the UV-Vis-NIR or Fourier transform infrared spectroscopy instruments).

Spectral curve deconvolution or multivariate curve resolution (MCR) methods are chemometric techniques concerning the extracting of the pure spectra and concentration profiles of the components in a chemical system operating in an evolutionary process.[22,23] Data analysis can be achieved by hard-modeling method where a chemical model is available or soft-modeling method where there is no robust idea about the model of the chemical reaction.[24-31]

This paper reports the investigation on the monomer formation process of the CoTSP in the presence of co-solvents and presents complete kinetic pathway obtained by

a recently proposed hybrid hard and soft-modelling multivariate curve resolution (HS-MCR) method applied to UV spectrophotometric data. This chemometric method can be applied to the simultaneous treatment of several experiments conducted under different experimental conditions. It allows the extraction of the pure spectra of the involved components together with their concentration profiles and, at the same time, it evaluates the kinetic model and their various rate constants.[32]

Solvent effect is closely related to the nature and extent of solute–solvent interactions developed locally in the immediate vicinity of solute. One key approach to understand solvent effects is the solvent-induced changes in the electronic transition of solutes and another way is molecular dynamics (MD) simulation. In our previous works, QSAR, MD simulation and effect of porphyrins and phthalocyanines on enzyme activity and structure were investigated.[33-37] In this paper, monomer formation of the CoTSP is reported and kinetic pathway is obtained by applied MCR method to UV spectrophotometric data. This work reports the effect of various co-solvents on the absorption spectra of Co(II)-phthalocyanine. Furthermore, the study is supplemented by MCR and MD calculations.

Experimental

Materials. Co(II)-phthalocyanine and used co-solvents; dimethyl formamide (DMF), acetonitrile (AN), dimethyl sulfoxide (DMSO) and ethanol (EtOH) were purchased from Merck Co. UV-Visible spectra were recorded on a SPECORD 205 Analitik-Jena spectrophotometer from 200 to 800 nm. In an investigation phthalocyanine was mixed with various concentration of solutions made in different solvent from 0 to 3.57 M.

Instruments. UV-Visible spectra were recorded on a SPECORD 205 Analitik-Jena spectrophotometer from 200 to 800 nm with a slit width of 5.0 nm: The sample cuvette contained the phthalocyanine in the distilled water and solvent while the reference cuvette only contained solvent.

Sample Preparation. Sodium salts of CoTSP, were obtained from Merck in the highest purity possible and was used as received. Scheme 1 shows the chemical structure of CoTSP.

Doubly distilled water was used for all the experiments. For optical absorption individual micromolar (30, 40 and 50 μM) phthalocyanine solutions were prepared and mixed with appropriate different value of solvents. For UV-Vis, all phthalocyanine solutions were mixed with all above cited solvents. So, three different stock solutions of CoTSP were prepared in water. The conversion of the phthalocynine into the various forms (monomer and dimer) was directly monitored by UV-vis spectroscopy in 1-cm quartz cells at room temperature. All experiments were repeated at least three times to check for reproducibility.

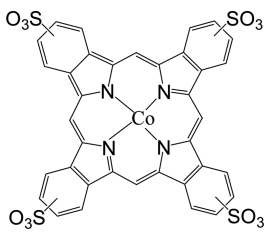

Scheme 1. Molecular structure of CoTSP.

MCR Calculations for Temperature Effect Spectra. Study of the CoTSP aggregation using multivariate curve resolution analysis of the visible absorbance spectra over a concentration range of 30, 40 and 50 μM was carried out in the presence of various solvent of AN, EtOH, DMF and DMSO. A hard modeling-based multivariate curve resolution method was applied to determine the dissociation constants of the CoTSP aggregates at various temperatures ranging from 25, 45 and 65 °C and in the presence of various solvents.

A chemical model was proposed for dissociation of CoTSP dimer as:

$$(\mathrm{CoTSP})_2 + 2\mathrm{Solvent} \xrightarrow{K} 2\mathrm{CoTSP} - \mathrm{Solvent}$$

$$K = \frac{[\mathrm{CoTSP} - \mathrm{Solvent}]^2}{[(\mathrm{CoTSP})_2][\mathrm{Solvent}]^2} \quad (1)$$

The above chemical model was used to study the dissociation of CoTSP in aqueous solution. A hard modeling-based multivariate curve resolution method was applied to analyze the spectrophotometric data at different temperatures, simultaneously, by which the dissociation constants of aggregates as well as the corresponding enthalpies and entropies were calculated. The steps taken in the employed hard-modeling method were as follows. In order to obtain values of dissociation constants of the aggregates, the concentration profile of monomer and dimer were calculated and using these profiles, dissociation constant of aggregates was obtained by solving the related relationships (Eq. 1). van't Hoff equation was used to calculate and compare the enthalpy and entropy changes. These calculations were also done to compare the solvent effect. In addition, two components were identified by factor analysis of the augmented data matrices. The recorded absorbance data through CoTSP aggregation process were first analyzed by the explained hard model method at fixed solvent (DMF) volume. A new study on the dissociation of CoTSP dimer using multivariate curve resolution analysis of the visible absorbance spectra over a concentration range of 30 to 50 μM was done. The resolved concentration profiles at three temperatures and in the presence of four studied solvents were obtained.

Multivariate Curve Resolution-alternative Least Squares (MCR-ALS). When a degradation process is monitored by UV spectroscopy, a series of spectra are collected. Changes in these spectra can be used to extract the analytical information necessary to resolve the system, including the pure spectra and concentration profiles of the single components and the kinetics parameters.

The recorded experimental data can be ordered in a data matrix **D**, whose rows (*r*) are the spectra at different times and whose columns (*c*) are the process signals at different wavelengths. Multivariate curve resolution (MCR) methods

decompose mathematically these data into the contributions due to the pure components of the system, following a bi-linear model derived from the generalized Lambert–Beer's[38] absorption law.

$$D_{(r\times c)} = C_{(r\times n)}S^{T}_{n\times c} + E_{r\times c} \quad (2)$$

Where C is the concentration of matrix on *n* components and S^T is the matrix of their spectra. E represents the unexplained variance in the data set. In MCR methods, the first step is the estimation of the number of involved components (*n*) in the kinetic system, which is initially obtained by application of singular value decomposition (SVD). Moreover, iterative MCR methods, like MCR-ALS, need a preliminary estimation of $\mathbf{S}^T$ or **C**, calculated either by evolving factor analysis (EFA), by selection of the pure variables, or by any previously estimation of them. These initial estimates are used to start the alternating least squares (ALS) constrained optimization through an iterative process. At each cycle, a new estimation of S^T and C is calculated by solving alternatively the two least-squares matrix equations.[39]

Molecular Dynamics Simulation. Simulations of phthalocyanine aggregation in the presence of water and co-solvents were carried out using the Gromacs package. The computer applied the Rocks cluster networking and Centos operating systems. The Calculations were done only by one trajectory of simulation and the repeated trajectory showed similar results. The latest versions of GROMACS 4.5.4 was run in parallel by the BirgHPC. A flexible SPC water model was used to describe the water molecules. The pre-optimized structures of CoTSP and solvents include AN, EtOH, DMF and DMSO, with Molecular Mechanics Force Field (MM+) and the Polak–Ribiere algorithm were obtained using Hyperchem 7 software until the root mean square gradient was 0.001 kcal mol^{-1}. Force field parameters and geometries were generated using PRODRG2 server (http://davapc1.bioch.dundee.ac.uk /cgi-bin/prodrg_beta) for CoTSP, DMF, AN, DMSO, and EtOH. All MD simulations were carried out using the GROMOS96 43al force field, at 300 K and one of the systems was simulated for 40 ns to ensure computation time. All of the simulations were equilibrated by 5 ns with position restraints on the phthalocyanine to allow for the relaxation of the solvent/co-solvent molecules. After equilibration, the molecular dynamic runs were 20 ns long. The non-bonded interaction was switched to zero at a cut-off of 9 Å with PME electrostatic. Within these production runs, the Nose–Hoover thermostat with a coupling constant of 0.5 fs, and the Parrinello–Rahman barostat with a coupling constant of 2.0 fs were utilized.

MD simulations were conducted for randomly distributed 100, 200, 300, 400 and 500 molecules of DMF, AN, DMSO, and EtOH in water as well as 5 and 8 CoTSP molecules at 300 K and 1 bar. In order to investigate the concentration effect, solvent was fixed and then water molecules were randomly added into the simulation box of 258 nm^3 and initial configurations were minimized using steepest descent algorithm with 5000 integration step. Variations of distance between the mass centers of CoTSP versus the time were averaged and calculated. The calculations were performed using 5 quad core parallel computers including 40 processor units.

Averaged data of distance between phthalocyanines were transferred in to Origin (version 5) software and were fitted by first order exponential growth to calculate dissociation rate constant. The conformational changes of the system during MD simulations were monitored by the root-mean-square derivations (RMSD) relative to its initial structure as a reference. The RMSD value, a measure of molecular mobility, is calculated by translating and rotating the coordinates of the instantaneous structure to superimpose the reference structure with a maximum overlap.[22] RMSDs were calculated, for the trajectories of the CoTSP, from the starting structures as a function of time. The simulation trajectories were analyzed using several auxiliary programs provided with the GROMACS package.

The radial distribution function $g(r)$ is the probability density of finding a particle at distance r from the reference particle. g(r) between particles of type A and B is defined in the following term:

$$g(r) = \frac{\langle\rho(r)\rangle}{\langle\rho_B\rangle_{\text{local}}} = \frac{1}{\langle\rho_B\rangle}\frac{1}{N_A}\Sigma_{j\in B}^{N_B}\Sigma_{j\in A}^{N_A}\frac{\delta(r_{ij}-r)}{4\pi r^2} \quad (3)$$

Where $\langle\rho(r)\rangle$ is the particle density of type B at a distance r around particles A, and $\langle\rho_B\rangle_{\text{local}}$ is the particle density of type B averaged over all spheres around particles A with radius r_{max}. Usually the value of r_{max} is half of the box length.[16] Distance of the molecules was defined by the distance separating the CoTSPs. The N_A, N_B and $\delta(r_{ij} - r)$ are number of A, B particles and kronecker delta.

Results and Discussion

Effects of Solvents on the Electronic Absorption Spectra. Co(II)-phthalocyanine is known to aggregate in water as a coplanar association of rings progressing from monomer to dimer. In studied co-solvents, AN, EtOH, DMSO and DMF, when solvent content increases, the intensity of the *Q* band also increases. Figure 1 depicts absorption spectra of phthalocyanine in the presence of AN. The intensity of the monomer peak is enhanced as compared to the peak arising from the aggregated species as shown in Figure 1.

Thus one can presume that most of the dye molecules are present in the monomeric form in cosolvents. On changing the solvent, the positions of the absorption peaks are shifted and indicate that the absorption wavelengths are sensitive to the environmental factors of the solvents. The Q band of the Co(II)-phthalocyanine molecule was red-shifted more than less polar solvent by increase of solvent polarity. Results of other co-solvents (obtained and not shown here) shows that the largest red shift (10 nm) of the Q band was observed for Co(II)-phthalocyanine in DMSO.

The shift to longer wavelength could be due to either the destabilization of the highest occupied molecular orbital (HOMO) or the stabilization of the lowest unoccupied molecular orbital (LUMO).[3] By increasing solvent molecules the

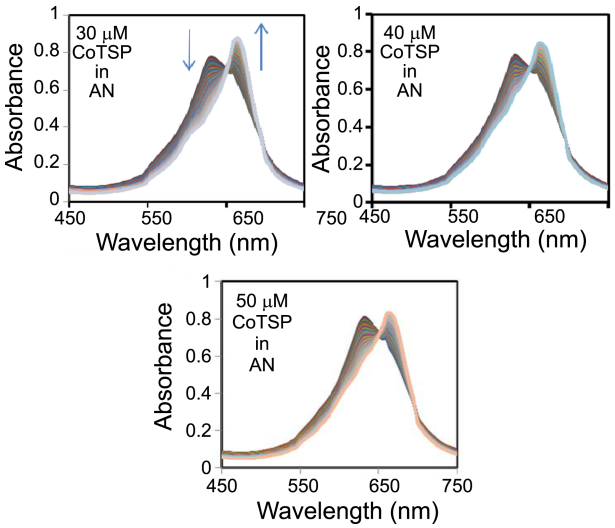

Figure 1. Absorption spectra of 30, 40 and 50 μM Co(II)-phthalocyanine in AN at different concentration range from 0 to 3.57 M.

band of dimer diminishes, and the band at 660 nm, which can be ascribed to the monomeric species, becomes more intense. The spectrum is typical for monomeric phthalocyanines showing Q-band at 660 nm. Again in polar solvents when solvent volume is increased, the intensity of the Q band also increased.

The changes in the effective absorptivity of 50 μM CoTSP at three different temperatures (*i.e.*, 25, 45 and 65 °C) are given in Figure 2. As it can be seen, the absorbance spectrum of the most diluted CoTSP solution, in which CoTSP is mainly present as monomeric species, is composed of a narrow band and a shoulder at 665 and 630 nm, respectively. As the number of solvent molecules is increased, the band at 630 nm is decreased and the band at 660 nm is increased. The changes are accompanied with the disappearance of the band at 630 nm.

These spectral changes are the evidence for the presence of monomer forms of CoTSP in the solutions. Similar results were obtained for temperatures of 25, 45, and 65 °C.

Multivariate Curve Resolution. Another attempt is made to provide more insight into the influence of the solvent on the tendency of CoTSP to aggregate. A UV–Vis molecular absorbance spectrum of CoTSP in the presence of co-solvent is presented in Figure 1. A cursory examination of the data presented in Figure 1 simply demonstrates the inter-conversion of two different forms of CoTSP within the temporal domain of the investigation. It is confirmed, therefore, that the evolution and decay of species within solvent-added aqueous CoTSP solutions is due to the presence of solvent. In the presence of solvent within the aqueous CoTSP solutions, the species corresponding to the absorbance band at 630 nm gradually changes to monomeric species (absorbance band at 665 nm) and clear isosbestic point is observed at 650 nm (Fig. 2).

As it can be seen, the absorbance spectrum of the most diluted CoTSP solution, in which CoTSP is mainly present as monomeric species, is composed of a narrow band and a shoulder at 660 and 630 nm, respectively. As the molecules number of cosolvent is increased, the band at 630 nm is decreased and the band at 660 nm is increased and this effect is more for higher temperature. The changes are accompanied with the disappearance of the band at 630 nm. These spectral changes are the evidence for the presence of two forms of CoTSP in the solutions.

In addition, two components were identified by factor analysis of the augmented data matrices. These detected species can be related to monomer and dimer forms of CoTSP. The recorded absorbance data through CoTSP aggregation process were first analyzed by the explained hard model method at fixed solvent (DMF) volume.

In water, CoTSP is known to be aggregated to dimer at high concentration levels in the absence of solvent. We conducted a new study on the aggregation of CoTSP using multivariate curve resolution analysis of the visible absorbance spectra over a concentration range of 0 to 50 μM.

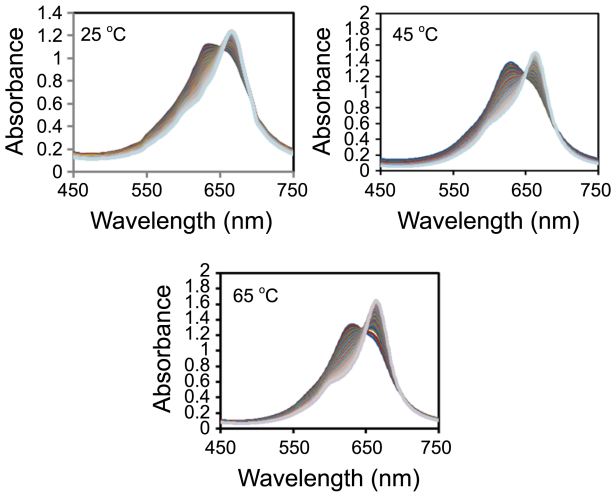

Figure 2. Plot of absorption spectra of aqueous 50 μM CoTSP solutions at three representative temperatures in the presence of 0 to 3.57 M of DMF.

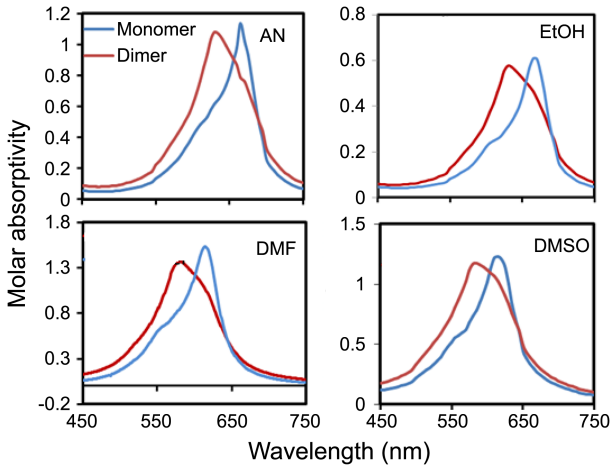

Figure 3. The resolved pure spectra of different CoTPPS aggregates at 25 °C. Left and right curves denote the dimer and monomer, respectively.

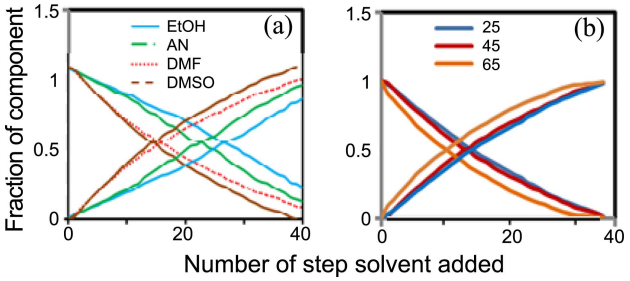

Figure 4. Fraction of component as a function of number of step, solvent added (a) in the various solvent with 50 μM concentration of dye and different concentration range of solvent and (b) in various temperatures of 25, 45, 65 °C in DMF.

Our results suggested the presence of at least two different species of principal components (PCs) in DMF solution.

The resolved spectral profile of the CoTSP aggregates, after convergence of the simultaneous hard modeling analysis of the absorbance-concentration data is presented in Figure 3. There is a very strong similarity between the resolved pure spectrum of CoTSP monomer and that recorded for the most diluted CoTSP solution, which contains mainly monomer species.

Figure 4 shows concentration profile of CoTSP aggregate as function of analytical concentration of solvent. The resolved concentration profile at three temperatures is given in this figure. It is observed that in the most solvent solution, CoTSP mainly exists as monomer and upon increasing the solvent volume, the monomeric form is evolved accompanied with a decrease in the amount of dimer.

In order to better describe the solvent effect, Values of K_d and solvent parameters are presented in Table 1. So, analysis of solvent effect on spectral properties of dye solutions was carried out by using the spectral shift in various solvents and correlating these with the solvatochromic parameters namely, π*(polarity–polarizability parameter), α (the solvents hydrogen bond donor ability), β (the solvents hydrogen bond acceptance ability), ε (permittivity) n (refractive index), μD (dipole moment) and K_d obtained from the literature.[40]

The correlation between K_d values and cited parameters were plotted in Figure 5. It shows that, K_d decreases with hydrogen bond donor property, while increases with other parameters. Also a good correlation between K_d and polarizabilty, dipole molent, dielectric constant is observed. So the main reason for the differences in K_d as can be seen in Table 1 can be ascribe to dipole moment (D) and dielectric constant of solvents.

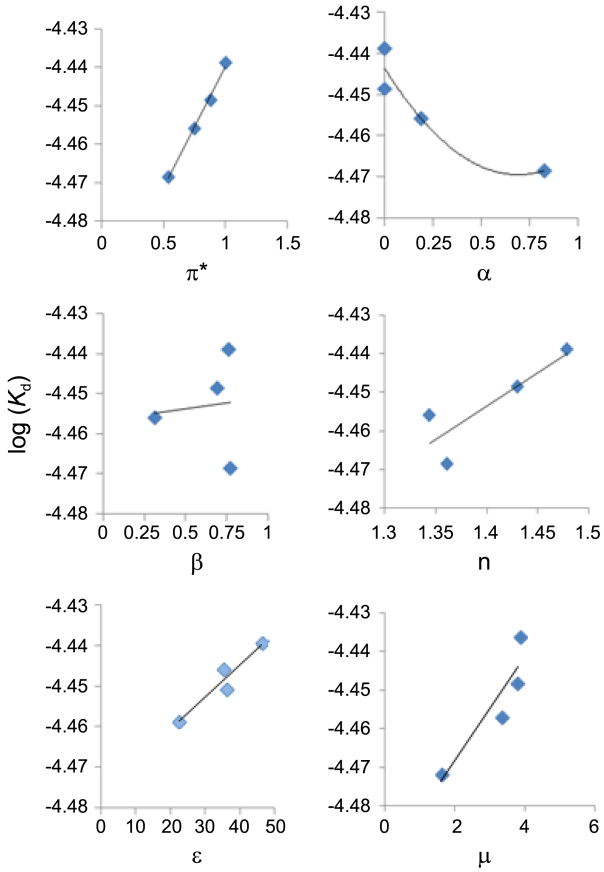

Figure 5. Correlation between solvent parameters obtained from ref. (Rauf, 2012) and dissociation constant (K_d).

The dissociation constant (K_d) of dimer aggregates for CoTSP in DMF at three different temperatures were presented in Table 2. Results of this table shows more K_d values of higher temperatures and more values of K_d in the presence of DMSO, DMF, AN, EtOH and water respectively which confirms above results.

Table 2. The calculated dissociation constant of dimer (K_d) aggregates for CoTSP in DMF at three different temperatures and concentration in DMSO

θ (°C)	K_d DMF (50 μM)	[CoTSP] (μM)	K_d DMSO (25 °C)
25	3.56×10^{-5}	30	3.90×10^{-5}
45	3.61×10^{-5}	40	3.73×10^{-5}
65	3.72×10^{-5}	50	3.64×10^{-5}

Table 1. Values of K_d and solvent parameters (Rauf, 2012)

Solvent	K_d	π*	α	β	n	ε	μ(D)
AN	3.50×10^{-5}	0.75	0.19	0.31	1.34	37.50	3.44
EtOH	3.40×10^{-5}	0.54	0.83	0.77	1.3614	24.55	1.69 = 1.66old
DMF	3.56×10^{-5}	0.88	0.00	0.69	1.4305	36.70	3.86
DMSO	3.64×10^{-5}	1.00	0.00	0.76	1.4790	47.2 = 46.68	3.96 = 4.1

In this table K_d, π*, α, β, *n*, ε, μ(D) denote dissociation constant, polarity, the solvents hydrogen bond donor ability, the solvents hydrogen bond acceptance ability, refractive index and dipole moment of the solvent)

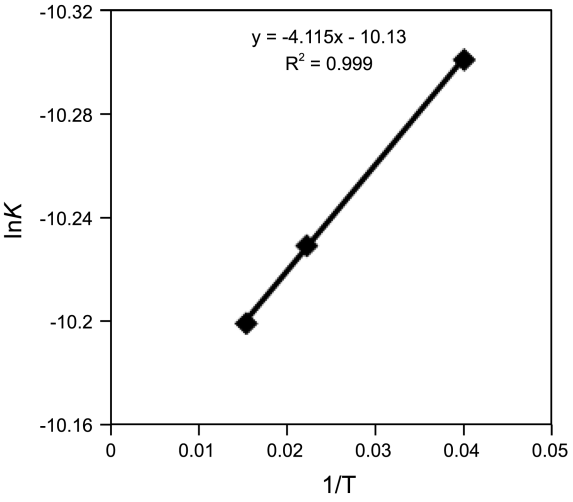

Figure 6. The plots of logarithm of dissociation constants against the inverse of temperature (van't Hoff equation) for the dissociation of CoTSP aggregates.

The estimated equilibrium constants at different temperatures can be used to calculate the thermodynamic parameters of the dissociation processes. If the standard enthalpy and entropy changes of a reaction (ΔH^{o} and ΔS^{0}, respectively) are not strongly dependent on the temperature, van't Hoff equation can be used to describe the relationship between equilibrium constant and temperature:

$$\ln K = -(\Delta H°/RT) + \Delta S°/R \quad (4)$$

Where, R is the universal gas constant and T is temperature in K. As shown in Figure 6, there is a well-defined linear relationship between the logarithm of dissociation constant and inverse of Kelvin temperature. The slope and intercept of the plots were used to calculate the standard enthalpy and entropy changes of dissociations, respectively. The calculated standard enthalpy and entropy changes of dissociation reactions were obtained as 34.214 kJ/mol and -84.279 J/mol.K respectively, in the presence of DMF.

For dissociation reaction, the enthalpy change is positive, which means that dissociation of aggregates to monomer is endothermic. On the other hand, the entropy change of dissociations is negative, which means that by dissociation of dimers or trimers to their monomer molecules the entropy of the system is decreased. This may seem to be surprising since, through dissociation, the number of CoTSP molecules in the products is larger than that of reactants. However, since we studied the system in aqueous solution, the relative number of solvent molecules surrounding the monomers and aggregates should be considered. Hydrophobic interaction is the main reason for aggregation of organic dye monomers in aqueous solutions.

Molecular Dynamics Simulation. MD simulation was employed to investigate the effects of solvent on phthalocyanine aggregation. Table 3 lists number of co-solvents and water molecules. Structure parameters include; g(r) and RMSD are obtained and averaged. Table 1 also notes that the monomer formation of phthalocyanine varies linearly with

Table 3. Number of co-solvent and water molecules used in the MD simulation

No. co-solvent	AN	EtOH	DMF	DMSO
100	8541	8725	8945	8874
200	8387	8689	8840	8716
300	8310	8602	8801	8637
400	8215	8564	8712	8542
500	8193	8312	8688	8384

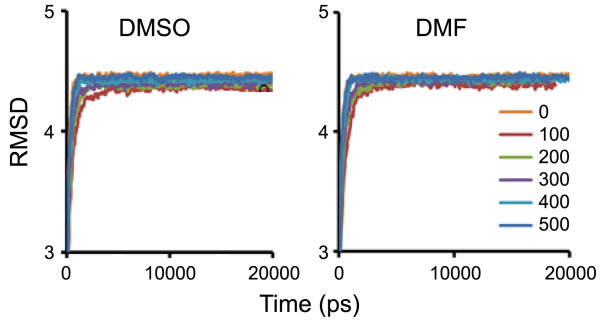

Figure 7. RMSD diagrams of system in the presence of various number of solvent molecules, AN, EtOH, DMF and DMSO.

the solvent dipole moment (D), dielectric constant polarizability parameter. An increase in polarizability, dipole moment (D) and dielectric constant values indicate that distance of molecules is increased with increasing capability of solvent to form monomer in solution.

RMSD curves were calculated, for the trajectories, from the starting structures of phthalocyanines as a function of time. Figure 7 shows the RMSD of five phthalocyanine molecules in the 20 ns in the presence of various number of solvent. In all of the systems, RMSDs reach a stable value within the first nanosecond of all the analyses.

It also shows that system has more structural changes in the presence of high number of solvent molecules. When solvent values increase, the RMSD and structural changes also increase.

Radial distribution function g(r) is a criterion for the distribution of atoms, molecules or other species around target species. The radial distribution function of phthalocyanines around each other *vs.* distance is shown in Figure 8 in various molecules of AN, EtOH, DMF and DMSO, respectively. The results show that as the number of solvent molecules increase, the $g(r)$ of phthalocyanines around each other decreases that is directly correlates with increasing polarizibility, dipole moment and dielectric constant.

Figures 8(e) and (f) compare g(r) for phthalocyanine in the 20 ns calculation in the presence of 100 and 500 molecules of cosolvents respectively.

The results show a decrease in g(r) by increasing the number of solvent molecules. It shows phthalocyanine aggregation at low concentration of solvent. These calculations revealed different tendencies of aggregate formations in the presence of four different solvents. The presence of four solvents causes the stabilization of phthalocyanine aggre-

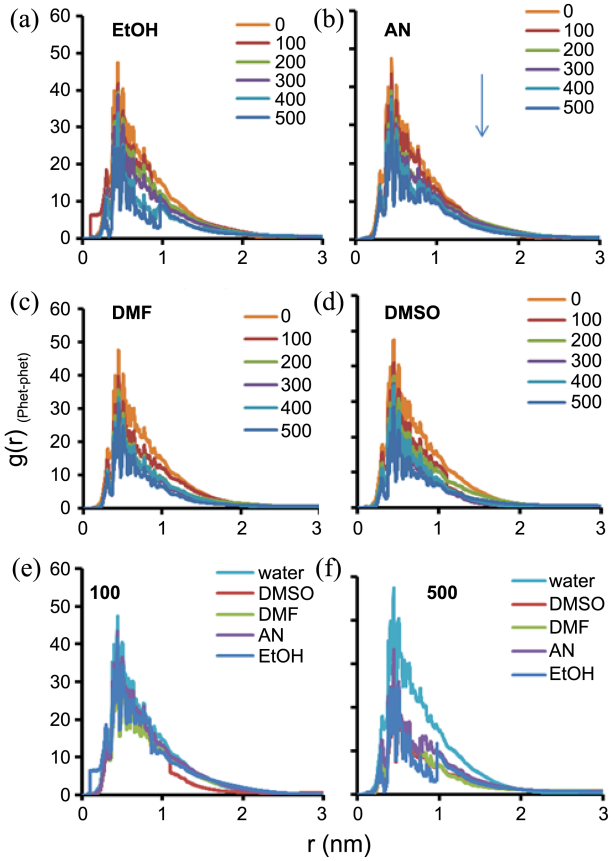

Figure 8. The radial distribution function of phthalocyanines around each other (g(r) $_{\text{phet-phet}}$) in different solvents and 20 ns calculation. The concentration of 100 and 500 molecules were given for comparison.

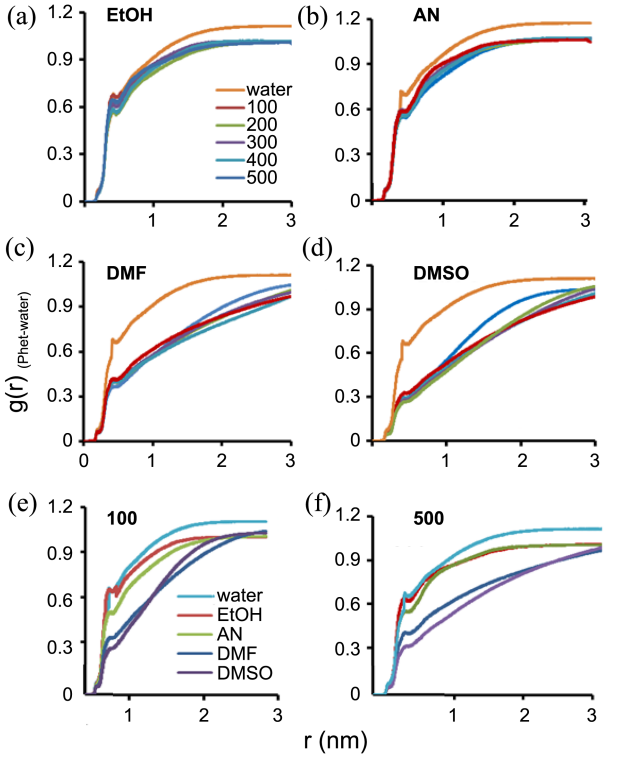

Figure 9. The g(r) of phthalocyanine-water in the 20 ns in the presence of 100 to 500 molecules of AN, EtOH, DMF and DMSO, respectively. Comparison g(r) of phthalocyanine-water in the 20 ns in the presence of 100 and 500 molecules of cosolvents.

gation, increase of hydration layer around phthalocyanine results in a self aggregation by an increase in the number of cosolvent molecules which is obvious in Figure 8.

The radial distribution function of water molecules around phthalocyanine is shown in Figure 9 in various number of cosolvent molecules AN, EtOH, DMF and DMSO, respectively.

From these figures, one can infer, in general, that as the number of AN and EtOH, DMF and DMSO increased, the g(r) of solvent around phthalocyanine decreased. In high number of solvent, all four solvents cause water exclusion from phthalocyanine and this effect is more for DMSO than EtOH. Existence probability of solvent around phthalocyanine in the presence of 100 to 500 EtOH is more than 100 to 500 DMSO. Results shows that water molecules are increased in hyrdation layer around phthalocyanine and this is due to solvent effect that become excluded from phthalocyanine-water surface. We can conclude from g(r) diagrams that a thin hydration layer is formed on phthalocyanine surface at low concentration of EtOH and this layer is reduced more in the presence of DMSO, DMF, AN and EtOH, respectively.

The last two parts of Figure 9 compare g(r) of phthalocyanine-water in the 20 ns in the presence of 100 and 500 molecules of co-solvents. Probability of occurrence of water around phthalocyanine is compared and this probability is more for EtOH, AN, DMF and DMSO respectively. As a consequence, DMSO causes more water exclusion from phthalocyanine.

The radial distribution function, g(r), of 100 to 500 AN, EtOH, DMF and DMSO around phthalocyanine *vs.* distance were obtained and results of comparison g(r) for phthalocyanine-cosolvent are shown for 100 and 500 molecules of solvents in last part of Figure 10 respectively. In order to explain this phenomenon we have used the exclusion and preferential hydration concepts. This is the reason for destabilizing effect of solvent. Solvent can decrease the hydration layer around phthalocyanine. This effect is due to exclusion of phthalocyanine from water/phthalocyanine surface. In this work preferential hydration has been investigated by analyzing the g(r) of DMSO, DMF, AN and EtOH - phthalocyanine. It can be seen that, by increasing DMSO, DMF, AN and EtOH numbers, phthalocyanine become solvated more and reduction of water molecules due to presence of more solvent is resulted. So it can be concluded that a thin hydration layer on phthalocyanine surface exist in systems with low concentration of DMSO, DMF, AN and EtOH, respectively.

The radial distribution function of five phthalocyanines in the presence of 500 molecules of EtOH and DMSO around phthalocyanine *vs.* distance was obtained during 40 ns and results of g(r) phthalocyanine-phthalocyanine, phthalocyanine-cosolvent and phthalocyanine-water are also shown in Figure

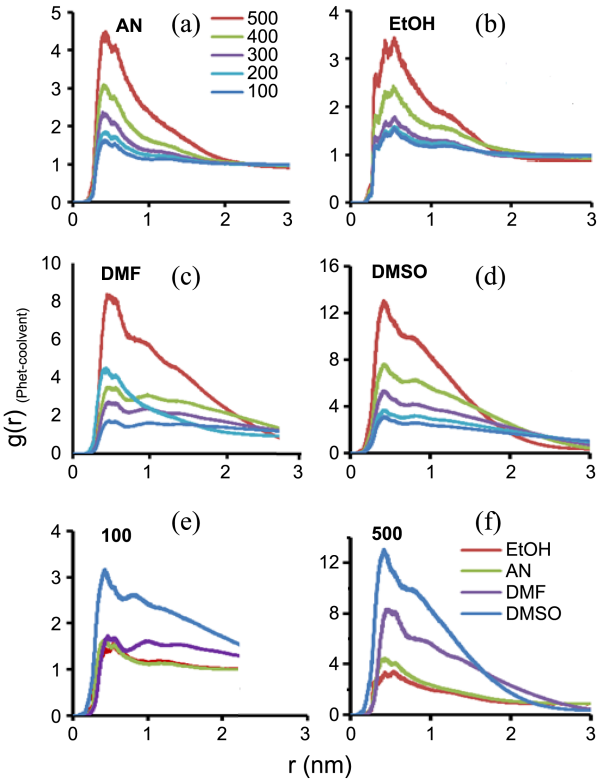

Figure 10. The *g*(r) of phthalocyanine-solvent in the 20 ns in the presence of 100 to 500 of (a) AN, (b) EtOH, (c) DMSO and (d) DMF respectively. (e) Comparison *g*(r) of phthalocyanine-water in the 20 ns in the presence of 100 and 500 solvent molcules.

11. Results of 40 ns simulation also confirm the above results that monomer formation decrease with addition of co-solvent. The results also confirm that as the polarizibility, dipole moment and dielectric constant of co-solvent increase the number of solvent molecules also increase. One of the above conditions such as aggregated configurations of five

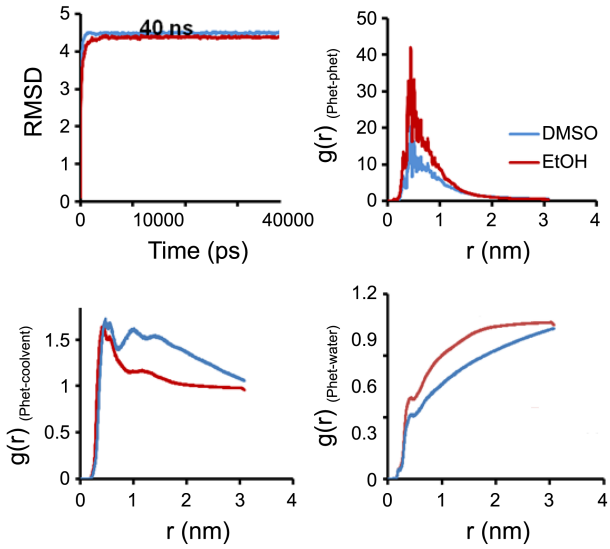

Figure 11. Comparison of *g*(r) 5 phthalocyanines in the presence of 500 DMSO and EtOH around phthalocyanine *vs.* distance.

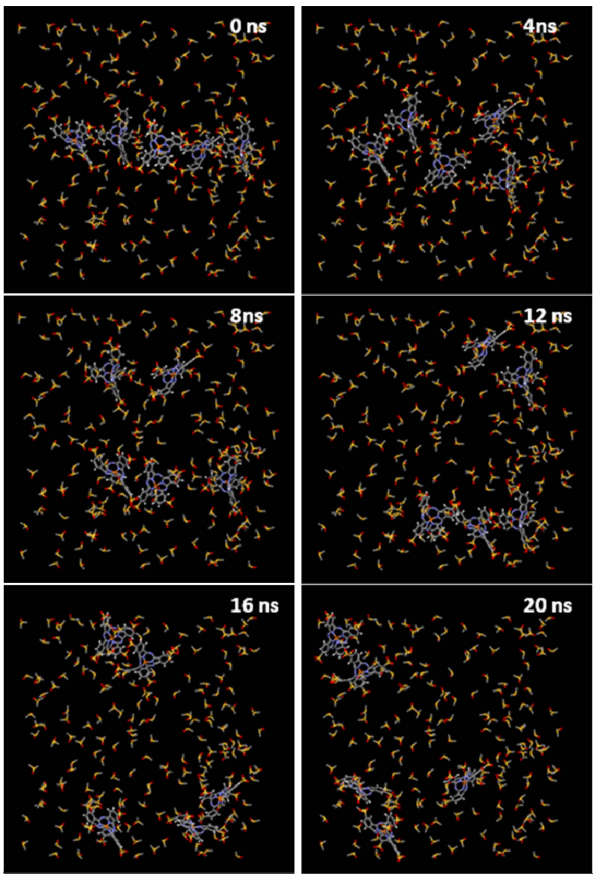

Figure 12. The molecular snapshot pictures obtained by DS Visualizer program for dissociation of aggregated CoTSP in the presence of 100 of DMSO solvent.

CoTPS molecules and 100 molecules of DMSO is selected. Then snapshots picture was taken by DS Visualizer program from configurations of the systems and result is presented in Figure 12. Water molecules are omitted from the figure for clarity.

The distance between centers of mass for CoTSP are evaluated as a function of simulation time and results are depicted in Figure 13. Increase of distance during simulation time indicating the more dispersion of CoTPS aggregates in the DMSO, DMF, AN and EtOH solution respectively which is obvious in following figure.

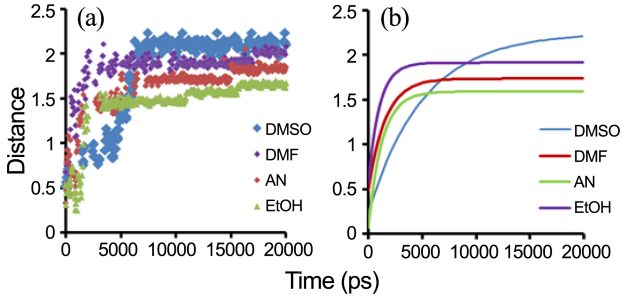

Figure 13. (a) Distance between CoTSP molecules during 20 ns MD simulation in different cosolvents (b) Fitted curves to exponential growth obtained by Origin 5 software.

Table 4. Relaxation times and rate constants of dye aggregation obtained from origin software from distance curves of Figure 13

Solvent	τ (ps)$^{-1}$	k (ps)
DMSO	5100.67	0.00019
DMF	3067.56	0.00033
AN	2284.37	0.00044
EtOH	914.18	0.00109

This figure shows increase of distance with time for the system which initial configuration used to be aggregated form. It means that distance between dye molecules increase in the presence of solvents and this effect is more in the presence of more polar solvents. The fitted diagrams have been shown for clarity and better comparison of solvent effect which have been obtained by Origin software. Table 4 has listed the value of rate constant (k) obtained from fitting distance with equation $D = D_o e^{-kt}$.

Conclusion

Solvent can have profound effects on phthalocyanine aggregation and function. The use of these solutions to stabilize or destabilize phthalocyanine aggregation, depending on the solvent, is commonplace. Destabilization, with different solvent, is one of the primary ways to assess phthalocyanine aggregation. Solvent may exert its effect by altering the solvent environment. The conversion of the phthalocynine into the various monomer form monitored by UV-vis spectroscopy and results indicated that by addition of co-solvent he intensity of the monomer peak is enhanced as compared to the peak arising from the aggregated species. CoTSP aggregated to dimer at high concentration levels in water and the aggregation is decreased at higher level of co-solvent and increases in higher temperatures. Multivariate curve resolution analysis used to obtain dissociation constant for aggregation and results revealed that dissociation constant was increased and then decrease by temperature and concentration of phthalocyanine, respectively. The enthalpy and entropy of the dissociation equilibriums were calculated utilizing the vant Hoff relation. Molecular dynamics simulation of co-solvent effect on CoTSP aggregation confirmed spectroscopy results. Structure analysis of MD results confirmed more effect of polar solvent to decrease monomer formation.

Acknowledgments. Publication cost of this paper was supported by the Korean Chemical Society.

References

1. Leznoff, C. C.; Lever, A. B. P. *Phthalocyanines-Properties and Applications*; VCH: Weinheim, 1989.
2. Hanack, M.; Subramanian, L. R. In *Handbook of Organic Conductive Molecules and Polymers*; Nalwa, H. S., Ed.; Wiley International: 1997; Vol. 687.
3. Wohrle, D.; Pomogailo, A. D.; Suvorova, O.; Tsaryova, O.; Dzardimalieva, G.; Baziakina, N. *Macromol Symp.* **2003**, *204*, 1-12.
4. Morishige, K.; Tomoyasu, S.; Iwani, G. *Langmuir* **1997**, *13*, 5184-5188.
5. Tominaga, T.; Hayashi, K.; Toshima, N. *J. of Porphyr. Phthalocya.* **1997**, *1*, 239-249.
6. Hofman, J. W.; Zeeland, F. V.; Turker, S.; Talsma, H.; Lambrechts, S. A. G.; Sakharov, D. V.; Hennink, W. E.; Van Nostrum, C. F. *J. Med. Chem.* **2007**, *50*, 1485-1494.
7. Ozoemena, K.; Kuznetsova, N.; Nyokong, T. *J. Photochem. Photobiol. A* **2001**, *139*, 217-224.
8. Ozoemena, K.; Kuznetsova, N.; Nyokong, T. *J. Mol. Catal. A* **2001**, *176*, 29-40.
9. Maree, S. E.; Nyokong, T. J. *J. of Porphyr. Phthalocya.* **2001**, *5*, 782-792.
10. Kolarova, H.; Nevrelova, P.; Bajgar, R. *Toxicol In Vitro* **2007**, *21*, 249-253.
11. Ben-Hur, E.; Chan, W. S. In *Porphyrin Handbook, Phthalocyanine Properties and Materials*; Kadish, K. M., Smith, K. M., Guilard, R., Eds.; Academic Press: 2003; Vol. 123.
12. Banfi, S.; Carous, E.; Buccafurni, L. *J. Organomet. Chem.* **2007**, *692*, 1269-1276.
13. Erdogmus, A.; Nyokong, T. *Dyes Pigments.* **2010**, *86*, 174-181.
14. Qiu, T.; Xu, X.; Qian, X. *J. Photochem. Photobiol. A* **2010**, *214*, 86-91.
15. Schnurpfeil, G.; Sobbi, A. K.; Spiller, W.; Kliesch, H.; Wohrle, D. *J. Porphyr. Phthalocya.* **1997**, *1*, 159-167.
16. Hale, P. D.; Pietro, W. J.; Ratner, M. A.; Ellis, D. E.; Marks, T. J. *J. A. Chem. Soc*. **1987**, *109*, 5943-5947.
17. Schlettwein, D.; Armstrong, N. R. *J. Phys. Chem*. **1994**, *98*, 11771-11779.
18. Meier, H.; Albrecht, W.; Wohrle, D.; Jah, A. *J. Phys. Chem*. **1986**, *90*, 6349-6353.
19. Law, W. F.; Liu, R. C. W.; Jiang, J.; Ng, D. K. P. *Inorganica Chimica Acta* **1997**, *256*, 147-150.
20. Levine, B.; Workman, *J. Anal. Chem.* **2008**, *80*, 4519-4531.
21. Hemmateenejad, B. *Chemometr. Intell. Lab. Syst.* **2006**, *81*, 202-208.
22. de Juan, A.; Tauler, R. *Crit. Rev. Anal. Chem*. **2006**, *36*, 163-176.
23. Malinowski, E. R. *Factor Analysis in Chemistry*; Wiley-VCH: Weinheim, 2002.
24. Rajko, R. J. *J. Chemometr.* **2009**, *23*, 172-178.
25. Hemmateenejad, B.; Javidnia, K.; Saeidi-Boroujeni, M. *J. Pharm. Biomed. Anal.* **2008**, *47*, 625-630.
26. Abdollahi, H.; Maeder, M.; Tauler, R. *Anal. Chem*. **2009**, *81*, 2115-2122.
27. Hemmateenejad, B.; Nezhad, M. R. H. *J. Phys. Chem. C*. **2008**, *112*, 18321-18324.
28. Chen, L. *Chemometr. Intell. Lab. Syst.* **2008**, *94*, 123-130.
29. Hemmateenejad, B. *J. Chemometr.* **2005**, *19*, 657-667.
30. Shamsipur, M.; Hemmateenejad, B.; Babaei, A.; Faraj-Sharabiani, L. *J. Electroanal. Chem.* **2004**, *570*, 227-234.
31. Blobel, J.; Bernado, P.; Svergun, D. I.; Tauler, R.; Pons, M. *J. Am. Chem. Soc.* **2009**, *131*, 4378-4386.
32. Shamsipur, M.; Hemmateenejad, B.; Akhond, M.; Javidnia, K.; Miri, R. *Pharm. Biomed. Anal.* **2003**, *31*, 1013-1019.
33. Ajloo, D.; Sangian, M.; Ghadamghahi, M.; Evini, M.; Saboury, A. A. *Int. J. Biol. Macromols.* **2013**, *47*, 47-61.
34. Ghadamgahi, M.; Ajloo, D. *J. Chem. Sci.* **2013**, *125*, 627-641.
35. Ghadamgahi, M.; Ajloo, D.; Moalem, M. *J. Porphyr. Phthalocya.* **2012**, *16*, 1082-1093.
36. Ajloo, D.; Hajipour, S.; Saboury, A. A.; Zakavi, S. *B. Korean Chem. Soc.* **2011**, *32*, 3411-3420.
37. Ghadamgahi, M.; Ajloo, D. *J. Porphyr. Phthalocya.* **2011**, *15*, 240-256.
38. De Juan, A.; Maeder, M.; Tauler, R. *Anal. Chim. Acta* **2001**, *442*, 337-350.
39. De Juan, A.; Tauler, R. *Anal. Chim. Acta* **2003**, *500*, 195-210.
40. Rauf, M. A.; Hisaindee, S.; Graham, J. P.; Nawaz, M. *J. Mol. Liq.* **2012**, *168*, 102-109.